Supplementary Information:

Effects of Surface Roughness on Droplet Impact Dynamics

Joe Ghossein[1,*], Chinmay Kendurkar[1], Jonathan B. Boreyko[2], and Olivier Coutier-Delgosha[1,3,†]

[1]Kevin T. Crofton Department of Aerospace and Ocean Engineering, Virginia Tech, Blacksburg, VA
[2]Department of Mechanical Engineering, Virginia Tech, Blacksburg, VA, USA
[3]CNRS, ONERA, Arts et Métiers ParisTech, Centrale Lille, FRE 2017 – LMFL, Laboratoire de Mécanique des Fluides de Lille, F-59000 Lille, France

June 16, 2026

Contents

S1 Statistical Robustness and Adjusted R^2 Analysis **2**
S1.1 Elastic Regime (We < 30) 2
S1.2 Inelastic Regime (We ≥ 30) 2

S2 Comparison with the Empirical Model of Singh et al. **3**

S3 Experimental Matrix **4**

S4 Impact Results **5**

* e-mail: joe20ghossein@vt.edu
† e-mail: ocoutier@vt.edu

S1 Statistical Robustness and Adjusted R^2 Analysis

To verify that the high predictive accuracy of our bimodal framework is not a result of overfitting, we performed an adjusted coefficient of determination (R^2_{adj}) analysis. This metric penalizes the model for the number of free parameters (k) relative to the number of data points (n), ensuring the scaling laws remain statistically robust and are not overly sensitized to the number of variables. The adjusted R^2 is calculated as:

$$R^2_{adj} = 1 - \left[\frac{(1 - R^2)(n - 1)}{n - k - 1}\right] \tag{1}$$

S1.1 Elastic Regime ($\mathbf{We < 30}$)

In the elastic regime, the model utilizes two independent fitting parameters: the prefactor κ and the geometric constant B_0 ($k = 2$). The data set for this regime consists of 10 experimental points from the current study and 60 data points from Singh et al.2021 (total $n = 70$).

- $n = 70$
- $k = 2$
- $R^2 = 0.91$
- $R^2_{adj} = 0.907 \approx 0.91$

S1.2 Inelastic Regime ($\mathbf{We \geq 30}$)

In the inelastic regime, where inertial and viscous effects dominate, the geometric constant B_0 is negligible, and the model relies on a single fitting parameter: the prefactor α ($k = 1$). This regime comprises 25 valid experimental data points (excluding shattering and splashing).

- $n = 25$
- $k = 1$
- $R^2 = 0.98$
- $R^2_{adj} = 0.978 \approx 0.98$

The negligible difference between R^2 and R^2_{adj} in both regimes confirms that the model is mathematically lean and the observed trends are driven by the underlying physical scaling rather than parameterization.

S2 Comparison with the Empirical Model of Singh et al.

To further show the robustness of our presented mode, we compare our experimental data for maximum spreading ratio ($\beta_{\max}$) against the empirical model proposed by Singh et al. 2021. The Singh model utilizes a power-law relationship incorporating the 1D roughness amplitude (R_{a}) and the Weber number:

$$\beta_{max} = 0.39 \left(\frac{We}{Oh}\right)^{0.1} \left(\frac{R_a}{D_0}\right)^{-0.065} \tag{2}$$

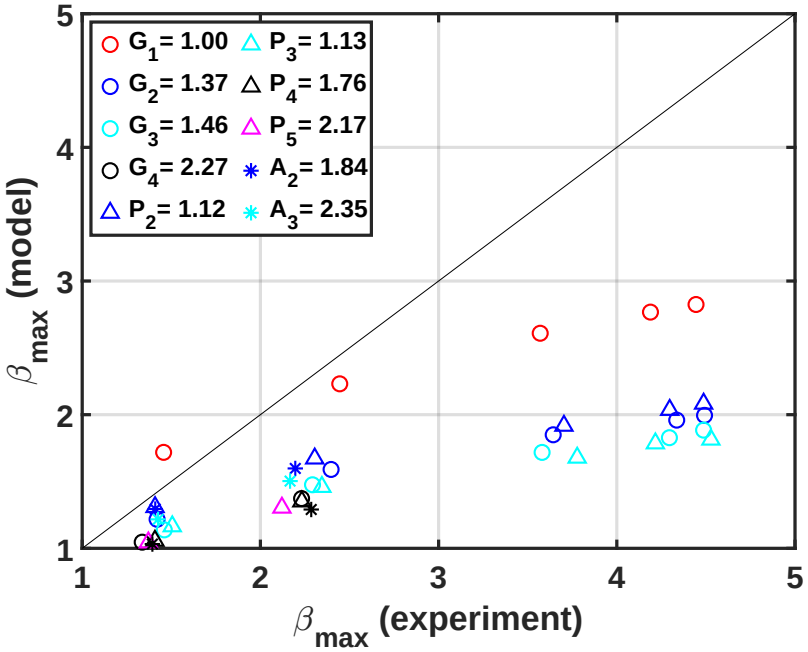

Figure S1: Comparison between experimental results and the empirical model proposed by Singh et al. The model exhibits a significant systematic under-prediction for spreading ratios $\beta_{\max} > 2$, failing to capture the inertial dynamics of high-velocity impacts. This deviation highlights the limited range of validity of empirical power-law fits compared to the physically grounded energy-balance framework proposed in this study.

As shown in Figure S1 the Singh model exhibits a significant systematic under-prediction of the experimental data, particularly for impacts where $\beta_{\max} > 2.5$. We attribute this discrepancy to three primary factors:

1. Restricted Spreading Regime: The Singh model was calibrated using a data set where the spreading ratio remained relatively low ($1 < \beta_{\max} < 2$). As evidenced by our data, the power-law scaling fails to capture the inertial dynamics of larger, 'pancake-like' impacts typical of higher Weber numbers (We > 100).

2. Roughness Descriptor: The model relies on the average roughness amplitude (R_{a}). As discussed in Section 2 of the main text, R_{a} is an amplitude-based metric that does not uniquely define the interfacial area ratio (r). Consequently, it cannot fully account for the Wenzel-state surface energy changes that govern spreading on complex topographies.

3. Absence of Energy Balance: Unlike the energy-based framework proposed in this study, the Singh model does not explicitly account for the partition of energy between surface creation and viscous dissipation. This leads to a 'plateau' effect in the model's predictions (Figure S1) that does not reflect the physical reality of continuous inertial spreading.

These results reinforce the necessity of a bimodal, energy-based framework to maintain predictive accuracy across diverse surface topographies and impact velocities.

S3 Experimental Matrix

Table S1: Laser printer settings used for glass surfaces

Glass				
Roughness (µm)	DPI	Power(%)	Speed	No. of Passes
0.012	0	0	0	0
2.37	1000	25	80	1
6.5	1000	50	80	1
22.49	1000	20	50	7

Table S2: Laser printer settings used for PETG surfaces

PETG				
Roughness (µm)	DPI	Power(%)	Speed	No. of Passes
1.18	1000	8	100	1
9.61	1000	10	100	2
31.33	400	25	80	4
55.04	100	40	60	7

Table S3: Laser printer settings used for aluminum surfaces

Aluminum				
Roughness (µm)	Frequency (Hz)	Power(%)	Speed	No. of Passes
2.21	20	50	90	1
5.71	20	90	90	1
58.31	20	100	20	6

S4 Impact Results

Table S4: Impact results for glass. Reported values for each data point correspond to mean values of three runs.

Glass						
Sample	D_0 **(mm)**	V_0 **(m/s)**	**We**	$\beta_{\mathbf{max}}$	Impact behavior	Droplet Ejection
	2.10	0.31	2.75	1.46	Staircase	No
	2.09	1.14	37.60	2.45	Deposition & Worthington Jet	No
1	2.17	2.41	173.06	3.57	Deposition	No
	2.13	3.32	319.96	4.19	Deposition	No
	2.10	3.71	396.94	4.44	Deposition	No
	2.09	0.31	2.74	1.42	Staircase	No
	2.09	1.18	39.61	2.39	Deposition & Worthington Jet	No
2	2.17	2.41	172.64	3.64	Deposition & Receding Breakup	No
	2.11	3.32	317.32	4.34	Receding Breakup	No
	2.09	3.71	393.65	4.49	Receding Breakup	No
	2.15	0.30	2.62	1.46	Staircase	No
	2.12	1.11	35.71	2.29	Deposition & Worthington Jet	No
3	2.14	2.35	161.32	3.58	Deposition	No
	2.11	3.26	305.63	4.30	Deposition & Negligible Splash	No
	2.12	3.76	410.42	4.49	Deposition & Negligible Splash	No
	2.04	0.31	2.67	1.34	Staircase	No
	2.09	1.17	39.41	2.23	Deposition	No
4	2.13	2.38	164.91	–	Shattering	No
	2.17	3.28	318.83	–	Shattering	No
	2.17	3.76	418.84	–	Shattering	No

Table S5: Impact results for PETG. Reported values for each data point correspond to mean values of three runs.

PETG						
Sample	D_0 **(mm)**	V_0 **(m/s)**	**We**	$\beta_{\mathbf{max}}$	Impact behavior	Droplet Ejection
	2.06	0.36	3.66	1.41	Staircase & Worthington Jet	Yes
	2.09	1.21	41.66	2.31	Staircase & Worthington jet	Yes
2	2.10	2.38	162.91	3.70	Deposition	No
	2.06	3.28	303.19	4.29	Deposition & Negligible Splash	No
	2.06	3.67	380.09	4.49	Deposition & Negligible Splash	No
	1.99	0.41	4.64	1.51	Staircase & Worthington Jet	Yes
	2.09	1.21	41.73	2.35	Deposition & Worthington Jet	Yes
3	2.11	2.41	167.79	3.78	Deposition & Receding Breakup	No
	2.09	3.32	314.34	4.22	Deposition & Receding Breakup	No
	2.05	3.67	376.65	4.53	Negligible Splash & Receding Breakup	No
	2.05	0.36	3.65	1.41	Staircase & Worthington Jet	No
	2.09	1.21	41.62	2.23	Deposition & Worthington Jet	No
4	2.09	2.41	167.11	-	Splashing	No
	2.09	3.32	315.82	-	Splashing	No
	2.11	3.76	407.28	-	Splashing	No
	2.03	0.41	4.2	1.37	Staircase & Worthington Jet	No
	2.11	1.21	41.93	2.12	Deposition	No
5	2.09	2.41	166.97	-	Splashing	No
	2.09	3.32	315.99	-	Shattering	No
	2.13	3.80	421.20	-	Shattering	No

Table S6: Test matrix results for aluminum. Reported values for each data point correspond to mean values of three runs.

Aluminum						
Sample	D_0 **(mm)**	V_0 **(m/s)**	**We**	$\beta_{\mathbf{max}}$	Impact behavior	Droplet Ejection
	2.08	0.41	4.85	1.41	Full Rebound	No
	2.09	1.18	39.65	2.19	Full Rebound	Yes
2	2.07	2.41	165.13	-	Shattering	No
	2.09	3.32	314.01	-	Shattering	No
	2.10	3.76	406.09	-	Shattering	No
	2.09	0.41	4.85	1.43	Full Rebound	No
	2.11	1.18	39.78	2.17	Full Rebound	Yes
3	2.09	2.35	158.46	-	Shattering	No
	2.12	3.32	318.64	-	Shattering	No
	2.01	3.76	388.48	-	Shattering	No
	2.08	0.39	4.25	1.39	Full Rebound	No
	2.09	1.18	39.50	2.29	Full Rebound	Yes
4	2.08	2.38	161.32	-	Shattering	Yes
	2.09	3.32	314.18	-	Shattering	No
	2.14	3.76	412.82	-	Shattering	No

References

R. K. Singh, P. D. Hodgson, N. Sen and S. Das, *Langmuir*, 2021, **37**, 3038–3048.